Synthesis, characterization and antibacterial activity of silver nanoparticles using *Rhazya stricta*

Adeeb Shehzad [1] , **Munibah Qureshi** [1] , **Saima Jabeen** [1] , **Rizwan Ahmad** [2] , **Amira H. Alabdalall** [3] , **Meneerah Abdulrahman Aljafary** [3] , **Ebtesam Al-Suhaimi** Corresp. [3, 4]

[1] Department of Biomedical Engineering and Sciences, School of Mechanical and Manufacturing Engineering, National University of Science and Technology, Islamabad, Pakistan

[2] College of Clinical Pharmacy, Imam Abdulrahman Bin Faisal University, Dammam, Saudi Arabia

[3] Department of Biology, College of Sciences, Imam Abdulrahman Bin Faisal University, Dammam, Saudi Arabia

[4] Institute for Research and Medical Consultations, Imam Abdulrahman Bin Faisal University, Dammam, Saudi Arabia

Corresponding Author: Ebtesam Al-Suhaimi
Email address: ealsuhaimi@iau.edu.sa

Background Green synthesis of metallic nanoparticles has gained significant attention in the field of nano-medicine due to environment-friendly and cost-effective alternative in comparison to other physical and chemical methods. Several metals such as silver, gold, iron, titanium, zinc, magnesium, and copper have been subjected to nano-formulation for a wide range of useful applications. Silver nanoparticles (AgNPs) are playing a major role in the field of nano-medicine and nanotechnology. They are widely used in diagnostics, therapeutic and pharmaceutical industries. Studies have shown potential inhibitory antimicrobial, anti-inflammatory and anti-angiogenesis activities of AgNPs. **Methods** AgNPs have been synthesized using silver nitrate (AgNO3) and methanolic root extract of *Rhazya stricta* that belongs to the *Apocynaceae* family. Stability and dispersion of nanoparticles were improved by adding xylitol. Synthesized nanoparticles were characterized by UV–vis spectroscopy, scanning electron microscopy (SEM), Energy dispersive spectroscopy (EDS), X-ray diffractometer (XRD), and Fourier transforms infrared spectroscopy (FTIR). Furthermore, the antibacterial effect of the plant extract and the nanoparticles were evaluated against gram-positive (*Bacillus subtilis*) and gram-negative (*Escherichia coli*) bacteria. **Results** The Average size of AgNPs synthesized, was 20 nm with the spherical shape. *Rhazya stricta* based nanoparticles exhibited improved antibacterial activity against both gram-positive and negative strains.

1   **Synthesis, characterization and antibacterial activity of silver nanoparticles using *Rhazya***

2   ***stricta***

3   Adeeb Shehzad[1], Munibah Qureshi[1], Saima Jabeen[1,] Rizwan Ahmad[2], Amira H. Alabdalall[3],

4   Meneerah Abdulrahman Aljafary[3], Ebtesam Al-Suhaimi[3, 4*]

5   The first two authors equally contributed to this work

6   [1]Department of Biomedical Engineering and Sciences, School of Mechanical and Manufacturing

7   Engineering, National University of Science and Technology, Islamabad, Pakistan

8   [2]College of Clinical Pharmacy, Imam Abdulrahman Bin Faisal University, Dammam, Saudi

9   Arabia

10   [3]Department of Biology, College of Sciences, Imam Abdulrahman Bin Faisal University,

11   Dammam, Saudi Arabia

12   [4]Institute for Research and Medical Consultations, Imam Abdulrahman Bin Faisal University,

13   Saudi Arabia

15   **Correspondence***

16   Ebtesam A Al-Suhaimi, Department of Biology, College of Sciences & Institute for Research and

17   Medical Consultations, Imam Abdulrahman Bin Faisal University, Saudi Arabia

18   Email: ealsuhaimi@iau.edu.sa   Tel: +966133332444

23 **Abstract**

24 **Background**

25 Green synthesis of metallic nanoparticles has gained significant attention in the field of nano-

26 medicine due to environment-friendly and cost-effective alternative in comparison to other

27 physical and chemical methods. Several metals such as silver, gold, iron, titanium, zinc,

28 magnesium, and copper have been subjected to nano-formulation for a wide range of useful

29 applications. Silver nanoparticles (AgNPs) are playing a major role in the field of nano-medicine

30 and nanotechnology. They are widely used in diagnostics, therapeutic and pharmaceutical

31 industries. Studies have shown potential inhibitory antimicrobial, anti-inflammatory and anti-

32 angiogenesis activities of AgNPs.

33 **Methods**

34 AgNPs have been synthesized using silver nitrate (AgNO3) and methanolic root extract of *Rhazya*

35 *stricta* that belongs to the *Apocynaceae* family. Stability and dispersion of nanoparticles were

36 improved by adding xylitol.   Synthesized nanoparticles were characterized by UV–vis

37 spectroscopy, scanning electron microscopy (SEM), Energy dispersive spectroscopy (EDS), X-

38 ray diffractometer (XRD), and Fourier transforms infrared spectroscopy (FTIR). Furthermore, the

39 antibacterial effect of the plant extract and the nanoparticles were evaluated against gram-positive

40 (*Bacillus subtilis*) and gram-negative (*Escherichia coli*) bacteria.

41 **Results**

42 The Average size of AgNPs synthesized, was 20 nm with the spherical shape. *Rhazya stricta* based

43 nanoparticles exhibited improved antibacterial activity against both gram-positive and negative

44 strains.

1. Introduction

Nanotechnology is a new, fascinating and fast growing revolution in the interdisciplinary fields including biomedical, therapeutics, diagnostics and materials science. Nanotechnology involves creation and manipulation of materials at the nano scale by altering their molecular structure (Rajasekharreddy & Rani, 2014). Different metals such as silver, gold, iron, titanium, zinc, magnesium and copper have been subjected to nano-formulation for a wide range of beneficial applications by adopting various physical, chemical and biological techniques (Ponarulselvam et al., 2012). Green synthesis is an alternative approach for synthesizing nanoparticles (NPs) using natural resources such as microorganisms and medicinal plants as reducing agents. NPs synthesized by the green method are highly stable, environmental friendly, biocompatible, cost effective, less toxic and safe for diagnostic and therapeutic purpose (Ponarulselvam et al., 2012; Rajasekharreddy & Rani, 2014; Verma & Mehata, 2016).

Silver based nano-materials play a major role in the field of nano-medicine and nanotechnology (Logeswari & Abraham, 2015). Several studies have also proved antimicrobial activity of AgNPs against several pathogenic and multidrug-resistant microorganisms (Singh et al., 2016). Various chemical and physical techniques have been reported for the synthesis of AgNPs, however many of those techniques require costly chemicals which are also toxic (Ahmad et al., 2017). Therefore, the synthesis of NPs by using plant isolated compound could be an attractive strategy in the field of nanotechnology as it offers several advantages such as cost-effective, eco-friendly, rapid synthesis and high yield.

Owing to huge medicinal properties of plants, herein, it is reported green technique for the synthesis of silver nanoparticles by using roots of *Rhazya stricta*. It is a small, glabrous, erect shrub that contains alkaloids, flavonoids and phenolic compounds (Bukhari et al., 2017). *Rhazya stricta*

68   is also known as Harmal, widely distributed in Saudi Arabia and South Asia (Bukhari et al., 2017;

69   Obaid et al., 2017). Seed oil from Harmal is considered a potential rich source of d-tocopherol, a

70   major form of vitamin E (Nehdi et al., 2016). It is used for treating numerous diseases such as

71   obesity, diabetes mellitus, sore throat, cardiovascular, metabolic, neurodegenerative diseases as

72   well as cancers (Alagrafi et al., 2017). It exhibits anti-oxidant, anti-carcinogenic, antimicrobial,

73   anti-dramatist, antihypertensive (VanBeek et al., 1985), antidepressant, anti-inflammatory,

74   antipyretic, antifungal and herbicidal activities (Alagrafi et al., 2017; Ali et al., 2000; Baeshen et

75   al., 2010; Lantero, 2014; Sarfaraz, 2012; Van Beek et al., 1985). Previously, gold nanoparticles

76   (AuNPs) synthesized with extract of *Rhazya stricta* displayed better anticancer activity against

77   MFC-7 cell lines (Baeshen, 2013). In this study, we have synthesized AgNPs by using root extract

78   of *Rhazya stricta* plant as a reducing agent along with xylitol (sugar). The synthesized AgNPs was

79   tested for antibacterial activity against gram-positive (*Bacillus subtilis*) and gram-negative bacteria

80   (*Escherichia coli*).

81

82   **2. Materials and Methods**

83   **2.1. Chemicals and reagents**

84   AgNO3 and xylitol were purchased with ≥99.0% purity from Sigma-Aldrich. De-ionized water

85   was used for reaction and Whatman filter papers (125mm) were used for the purification and

86   filtration.

87   **2.2. Preparation of root extract**

88   *Rhazya stricta* was collected from southern part of Pakistan and identified in Taxonomy lab,

89   Department of Botany at Arid Agriculture University Rawalpindi Pakistan. The voucher specimen

90   number MAQ.2014.B313, was deposited in Department Herbarium of Botany, Arid Agriculture

91   University Rawalpindi. The roots of the plant were washed thrice with de-ionized water and shade

92   dried. Extracts were prepared by soaking 147 g of dried roots in 80% methanol at room temperature

93   for three days, and then filtered using Whatman filter paper (125mm). The solvent was evaporated

94   using a rotary evaporator. The resulted extract after drying was 13g.

95

96   **2.3. Biosynthesis of silver nanoparticles**

97   For the synthesis of AgNPs, 10 g of dried extract was dissolved in 18mL methanol and placed at

98   4°C. 1mM solution of $AgNO_3$ was prepared in deionized water. 6mL methanol-extracted plant

99   roots were added drop by drop in 100ml $AgNO_3$ (1mM) with continuous shaking. Another reaction

100   was carried out using the same amount of extract and 100mL of $AgNO_3$ with 6mL xylitol (10^{-2}

101   M). Then both reactions were heated separately using a magnetic stirrer at 60 °C for two hours.

102   The change in color was the indication for synthesis of NPs **[Fig. 1].**

103   For characterization of AgNPs, the sample was centrifuged for 20 minutes at 12000rpm.The

104   supernatant was discarded to get rid of any uncoordinated material. The Sample was then washed

105   thrice with distilled water to eliminate extra proteins or enzymes. After sonication, the sample was

106   dried with a vacuum drier for an overnight at 50°C.

107

108   **2.4. UV-Visible Absorbance spectroscopy**

109   Bio-reduction of Ag^+ ions in AgNO3 solution was observed by ultraviolet-visible (UV-Vis)

110   spectroscopy (UV-2800, BMS). UV spectrums for 250μl, 350μL, 450μL, 550μL, 650μL

111   concentrations of plant extract in 10mL of AgNO3 solution were monitored. The UV-Vis

112   absorption spectra for AgNPs was observed in a range of 300-600nm with UV-2800

113   spectrophotometer.

114 **2.5. Fourier Transform Infrared Spectroscopy (FTIR)**

115 Biomolecules responsible for reducing Ag^+ were analyzed by Fourier transform infrared (FTIR)

116 spectrometer. FTIR spectroscopy is an experimental technique used for analysis of functional

117 groups, molecular structure and chemical bonding of organic and inorganic samples, by producing

118 an infrared absorption spectrum (Perklin Elmer Spectrum 100) (Verma & Mehata, 2016).

119

120 **2.6. X-ray Diffraction (XRD)**

121 The structural characterization and crystalline nature of AgNPs were determined by X-ray

122 diffractometer (D8 Advance, Bruker) for the vacuumed dried AgNPs (Ashraf et al., 2016).

123

124 **2.7. Scanning Electron Microscopy (SEM)**

125 The size and morphology of AgNPs were investigated using JEOL-6490A-JSMScanning Electron

126 Microscope. Elemental composition of AgNPs was determined by Energy Dispersive

127 Spectroscopy (EDS).

128

129 **2.8. Antibacterial Activity**

130 The antibacterial activity of the extract and AgNPs was evaluated against *Escherichia coli*, and

131 *Bacillus subtilis* using disk diffusion method (Hu et al., 2017). Disks were soaked with distilled

132 water (negative control), standard antibiotic cefipime (positive control) with the trade name of

133 maxipime (glaxosmithkline), *Rhazya stricta* extract and the AgNPs solution with and without

134 xylitol addition separately. 50µL concentration of AgNPs was used to ensure identification of

135 antibacterial activity. Then the plates were incubated for 24-48 hours at 37°C and zone of

136 inhibition was measured for both bacterial strains.

137

3. RESULTS

3.1. UV-VIS Spectroscopy

140 Synthesis of nanoparticles started after the addition of root extract of *Rhazya stricta* into an

141 aqueous solution of AgNO3. The change in color from pale yellow to orange brown after 2 hours

142 heating (60°C) on magnetic stirrer indicated the formation of reduced silver [**Fig. 2A**].

143 To examine further AgNPs in aqueous suspensions, UV-Vis spectroscopy was used. As shown in

144 the **Fig. 2B**, the absorption peaks of AgNPs synthesized by *Rhazya stricta* root extract were

145 detected at 380, 392, 402, 414 and 427nm wavelength. The increasing concentration of plant

146 extracts also increased the broadening of the peak indicating the increased size of NPs. Previous

147 studies indicated that the spherical AgNPs have absorption bands at around 400 nm in the UV

148 visible spectra (Nasir, Mohammed, & Samir, 2016). These results indicate that the spherical

149 AgNPs have absorption bands at around 402 nm in the UV visible spectra. Thus, it can be reported

150 that particle size of AgNPs is highly subjective to the concentration of root extract.

151

3.2. SEM

153 For further confirmation, the size and shape of AgNPs, SEM was performed. **Fig. 3A and B** depict

154 the formation of spherical shape NPs. It was noticed that AgNPs synthesized only with plant

155 extract have shown more agglomeration [**Fig.3A**], while those synthesized with the addition of

156 xylitol were not agglomerated, well dispersed and with average particle size of 20 nm.

3.3. Elemental analysis

158 The AgNPs synthesized using *Rhazya stricta* were also characterized by EDX analysis, which

159 further confirmed the reduction of silver ion. The Optical absorption peak was recorded almost at

160 3 keV, which is obvious for silver nano-crystals absorption because of surface Plasmon resonance

161 [**Fig. 4**]. The EDX spectrum has shown silver peak along with oxygen and chlorine peaks. The

162 chlorine and oxygen peaks were may be attributed to glass biomolecules that were present on the

163 surface of silver nanoparticles or to chlorine on the glass slides that were used for sample

164 preparation [**Fig. 4**].

165

166 **3.4. XRD**

167 The dry powders of AgNPs synthesized with root extract of *Rhazya stricta* were subjected to XRD

168 analysis. XRD patterns of synthesized AgNPs are shown in **Fig.5**. The synthesized NPs were of

169 crystalline nature. The XRD pattern has shown the intense five peaks of NPs at 31.99, 45.5, 54.85,

170 57.52 and 67.24, were indexed to face-centered cubic structures of AgNPs. The XRD peaks

171 revealed that AgNPs formed using *Rhazya stricta* root extract were crystalline and spherical in

172 shape. The average nano size was confirmed by applying Debye–Scherrer formula $D = K\lambda / \beta\cos\theta$

173 which was found to be 20 nm.

174

175 **3.5. FTIR**

176 FTIR spectroscopy was used to investigate. FTIR analysis was done to identify biomolecules that

177 are responsible for Ag+ ions reduction and capping of biologically reduced AgNPs synthesized by

178 *Rhazya stricta* root extract along with xylitol. **Fig.6A** shows the FTIR spectrum of xylitol

179 displayed bands at 3362.59 (OH of alcohol) and 1417.88 (C-H bending of alkane). **Fig.6B** shows

180 the FTIR spectrum of root extract of *Rhazya stricta* plant that is showing peaks at 724, 1024, 1455,

181 1687, 2123, 2921 and 3374cm^{-1}. A peak at 3374cm^{-1} indicated stretching of the N–H bond of

182 amino groups and presence of attached hydroxyl (-OH) group. The absorption peaks at 2921 cm^{-1}

183   could be due to stretching of –CH functional groups. The peak at 1687 cm^{-1} corresponds to C–O

184   stretching in the carboxyl attached to the amide linkage in amide I. The absorption band at 1455

185   indicated the presence of C-N stretching in amide. The two bands present at 1024 and 742cm^{-1}

186   could be indicative of the –O– stretching vibrations of aromatic and aliphatic amines (Gou et al.,

187   2015). **Fig.6C** and **Fig**. **6D** show FTIR spectra for AgNPs synthesized using only *Rhazya stricta*

188   plant and along with xylitol.

189

190   **3.6. Antimicrobial activity of AgNPs**

191   Plant mediated synthesis of AgNPs exhibited tremendous antibacterial activity against various

192   bacterial strains. For this purpose, the antibacterial activity of AgNPs was examined with various

193   concentrations of root extract against *Bacillus subtilis* for gram-positive and *Escherichia coli* for

194   gram-negative strains. As shown in the **Fig.7A, and C**, three different concentrations (450µL,

195   550µL and 650µL) of plant extract in 10mL of AgNO3 were used to test the antibacterial activity.

196   When concentration was increased from 450µL to 550µL, the zone of inhibition also increased,

197   however, at 650µL, zone of inhibition was observed smaller than 550µL (**Fig. 7A and C**). The

198   positive control 10 mM of cefipime exhibited maximum zone of inhibition, whereas distilled

199   water, the negative control shown no inhibition on both strains (**Fig. 7B and D**). The AgNPs

200   synthesized by *Rhazya stricta* root extract along with xylitol displayed better antibacterial activity

201   as compared to plant extract only, because xylitol increased the stability and decreased the

202   agglomeration of synthesized AgNPs. Thus, uniform distribution of NPs enhanced the antibacterial

203   activity of synthesized AgNPs with root extract of *Rhyza stricta.*

204

205 **3.7. Time-dependent effect of AgNPs**

206 Once the concentration-dependent effect was confirmed, the effect of AgNPs synthesized using

207 *Rhazya stricta* root extract was examined for its time dependent activity. The 550 µL of AgNPs

208 with *Rhazya stricta* root extract was tested further with and without xylitol against *bacillus subtilis*

209 (gram-positive) and *Escherichia coli* (gram-negative). As shown in **Fig.8A** and **B,** AgNPs with

210 *Rhazya stricta* root extract and xylitol have shown an increased zone of inhibition as compared to

211 their individual zone of inhibition. These results confirm the enhanced antibacterial effect of

212 AgNPs synthesized with *Rhazya stricta* root extract and xylitol.

213

214 **3.8. Differential effect of AgNPs against gram-negative and positive pathogens**

215 The synthesized silver nanoparticles had more inhibition effect on *Escherichia coli* as compared

216 to *Bacillus subtilis* as shown in **Fig. 9A and B**. These results further confirmed that AgNPs

217 synthesized with *Rhazya stricta* root extract have better bactericidal effects against gram-negative

218 strains as compared to gram-positive strains.

219

220 **4. DISCUSSION**

221 Green synthesis of AgNPs could significantly overcome the problem of using chemical agents that

222 cause various adverse effects. Therefore, green synthesis of NPs is environment-friendly approach

223 (Gan & Li, 2012; Wang et al., 2017). *Rhazya stricta* plant roots possess antibacterial activity that

224 is considerably enhanced after incorporation with NPs. The characterization techniques advocated

225 the stability of the synthesized AgNPs. Experimentally, Xylitol has not the ability to reduce silver

226 ions, but it is possibly involved in the capping of the synthesized AgNPs by electrostatic attraction

227 or binding with the protein groups present in the extract through hydrogen bonding and enhanced

228   the silver nanoparticle's stability. It also protected the NPs from agglomeration (Kaviya et al.,

229   2011). Synthesis of the AgNPs starts with the change in color from pale yellow to orange brown

230   upon the addition of *Rhazya stricta* root extract [**Fig. 2A**]. It has been reported that excitation of

231   surface Plasmon resonance is responsible for yellowish brown color of AgNPs in aqueous solution

232   (Kaviya et al., 2011). This surface Plasmon vibration confirmed the biotransformation from an

233   ionic form to silver particles (Huang et al., 2007). Upon addition of *Rhazya stricta* root extract in

234   the aqueous solution of AgNO3 and xylitol, the color changed from pale yellow to orange brown

235   due to reduction of silver ion [**Fig. 2A**]. It was also noticed that increase in the concentration of

236   root extract in the synthesis reaction, increases the particle size. Further increase in plant extract

237   concentration shown noisy and broadened peak at UV-Vis spectrum. Current XRD results of

238   synthesized AgNPs with root extract of *Rhazya stricta* confirmed the structure of AgNPs as face-

239   centered cubic (fcc) with crystalline nature (Li et al., 2012). The EDX spectrum has shown clear

240   silver signal along with weak oxygen and chlorine peak, which might be due to the interaction and

241   binding of biomolecules to the surface of AgNPs (Kalainila et al., 2014).

242   FTIR analysis was performed to confirm that the bio-compounds involved in the reduction of ionic

243   and capping of the reduced AgNPs synthesized by *Rhazya stricta* root extract along with xylitol.

244   **Fig. 6A** shows FTIR spectrum of xylitol, it gave bands at 3362.59 (OH of alcohol) and 1417.88

245   (C-H bending of alkane). **Fig. 6B** represents the FTIR spectrum of root extract of *Rhazya stricta*

246   plant; it gave peaks at 724,1024, 1455,1687, 2123,2921 and 3374cm^{-1}.These peaks are expected

247   to be related with amide I shift due to carbonyl stretch in proteins (1687cm^{-1}), –C–H– stretch of

248   amine (2921 cm^{-1}), C–N stretching vibration of amine (1455 cm^{-1}), and –O– stretching vibrations

249   of aliphatic and aromatic amines (1024 and 742cm^{-1}), respectively (Gou et al., 2015; Wang et al.,

250   2017). A peak at 3374cm^{-1} indicated the stretching of the N–H bond of amino groups and shown

251   the presence of bonded hydroxyl (-OH) group (Gou et al., 2015; Hu et al., 2017; Wang et al.,

252   2017). After the formation of AgNPs peaks were shifted to little higher wavenumber as compared

253   to plant extract as indicated by **Fig. 6C**. Xylitol did not reduce the silver ions in the solution, but

254   it was used to cap/coat the synthesized AgNPs through electrostatic attraction or hydrogen bonding

255   with protein groups that further aided in more stability and better dispersion of NPs **Fig. 6D**. FTIR

256   spectrum of the *Rhazya stricta* roots extract confirmed the presence of carboxyl (-C=O), hydroxyl

257   (-OH) and amine (N-H) groups of *Rhazya stricta* roots extract and further revealed their

258   involvement in the reduction of silver ion to metallic silver nanoparticles (Nasir, Mohammed, &

259   Samir, 2016). Plant extract contains proteins that cap the silver nanoparticles through carboxyl or

260   amino group present in protein (Kaviya et al., 2011). It is believed that proteins of the root extract

261   of *Rhazya stricta* could bind to AgNPs through either free amino or carboxyl groups (Nasir et al.,

262   2016). The presence of the residual plant extract in the sample is due to the similarity of the spectra

263   with little marginal shifts in peak position (Saiqa, 2015). Thus these results have shown that the

264   functional groups of bio-compounds present in the root extract of *Rhazya stricta* have key role in

265   the reduction as well as capping of AgNPs.

266   Previous studies have also reported the antibacterial activity of AgNPs against gram negative and

267   gram positive strains of bacteria (Singh et al., 2008). It is well recognized that the antibacterial

268   effect of AgNPs is size and dose dependent. The results were supported by previously reported

269   studies (Sana & Dogiparthi, 2018), which have shown that AgNPs have more potential against

270   gram-negative bacteria then gram positive bacteria (**Fig. 7A and C).** Increase in the size of NPs

271   reduced their antibacterial activity (Kaviya et al., 2011). *Rhazya stricta*-AgNPs exhibited strong

272   antioxidant and antibacterial effects It is also concluded that the antibacterial activity of AgNPs

273 depends on the concentration of root extract and quantity of AgNPs in the medium (Rauf et al.,

274 2016).

275

276 **Conclusion**

277 AgNPs synthesized using *Rhazya stricta* root extract along with xylitol have shown potential

278 antimicrobial activity because they were mono dispersed, stable and have less aggregation. Plant

279 acted as a reducing agent in the synthesis of AgNPs and xylitol enhanced the dispersion of

280 nanoparticles. Smaller size of NPs displayed better antibacterial activity. Antibacterial activity of

281 *Rhazya stricta* plant root was enhanced when it was incorporated with AgNPs synthesis. Thus,

282 synthesized AgNPs increases the therapeutic efficacy, strengthen the medicinal values of *Rhazya*

283 *stricta* and provides a potent source of an antimicrobial agent against gram positive and gram

284 negative organisms. Future studies are needed to uncover the underlying mechanism of

285 bacteriostatic or bactericidal effects of green synthesized AgNPs.

286
287
288
289
290
291
292
293
294
295
296
297
298
299
300
301
302
303
304
305

306

307   **References**

308   Ahmad, A., Wei, Y., Ullah, S., Shah, S. I., Nasir, F., Shah, A., … Yuan, Q. (2017). Synthesis of

309   phytochemicals-stabilized gold nanoparticles and their biological activities against bacteria

310   and Leishmania. *Microb Pathog*, *110*, 304–312.

311   https://doi.org/10.1016/j.micpath.2017.07.009

312   Alagrafi, F. S., Alawad, A. O., Abutaha, N. M., Nasr, F. A., Alhazzaa, O. A., Alharbi, S. N., …

313   Wadaan, M. A. (2017). In vitro induction of human embryonal carcinoma differentiation by

314   a crude extract of Rhazya stricta. *BMC Complement Altern Med*, *17*(1), 1–13.

315   https://doi.org/10.1186/s12906-017-1852-7

316   Ali, B. H., Al-Qarawi, A. A., Bashir, A. K., & Tanira, M. O. (2000). Phytochemistry,

317   pharmacology and toxicity of Rhazya stricta Decne: A review. *Phytother. Res*, *14*(4), 229–

318   234. https://doi.org/10.1002/1099-1573(200006)14:4 HYPERLINK

319   Ashraf, J. M., Ansari, M. A., Khan, H. M., Alzohairy, M. A., & Choi, I. (2016). Green synthesis

320   of silver nanoparticles and characterization of their inhibitory effects on AGEs formation

321   using biophysical techniques. *Scientific Reports*, *6*(February), 1–10.

322   https://doi.org/10.1038/srep20414

323   Baeshen, N. A., Lari, S. A., Doghaither, H. A. R. Al, & Ramadan, H. A. I. (2010). Effect of

324   Rhazya stricta extract on rat adiponectin gene and insulin resistance, *6*(12), 1237–1245.

325   Baeshen MN. 2013. The effect of biosynthesized Rhazya stricta leaf extracts with gold

326   nanoparticles on breast cancer cell lines. *Biological systems* 5:1110–1118. DOI:

327   10.1039/c3ib40053k.

328   Bukhari, N. A., Al-Otaibi, R. A., & Ibrahim, M. M. (2017). Phytochemical and taxonomic

329   evaluation of Rhazya stricta in Saudi Arabia. *Saudi J Biol Sci*, *24*(7), 1513–1521.

330   https://doi.org/10.1016/j.sjbs.2015.10.017

331   Gan, P. P., & Li, S. F. Y. (2012). Potential of plant as a biological factory to synthesize gold and

332   silver nanoparticles and their applications. *Rev. Environ. Sci. Biotechnol*, *11*(2), 169–206.

333   https://doi.org/10.1007/s11157-012-9278-7

334   Gou, Y., Zhou, R., Ye, X., Gao, S., & Li, X. (2015). Highly efficient in vitro biosynthesis of

335   silver nanoparticles using Lysinibacillus sphaericus MR-1 and their characterization. *Sci*

336   *Technol Adv Mater*, *16*(1). https://doi.org/10.1088/1468-6996/16/1/015004

337   Hu, G., Liang, G., Zhang, W., Jin, W., Zhang, Y., Chen, Q., … Zhang, W. (2017). Silver

338   nanoparticles with low cytotoxicity: controlled synthesis and surface modification with

339   histidine. *J. Mater. Sci*, *53*(7), 1–13. https://doi.org/10.1007/s10853-017-1940-6

340   Huang, J., Li, Q., Sun, D., Lu, Y., Su, Y., Yang, X., … Chen, C. (2007). Biosynthesis of silver

341   and gold nanoparticles by novel sundried Cinnamomum camphora leaf. *Nanotechnology*,

342   *18*(10). https://doi.org/10.1088/0957-4484/18/10/105104

343   Kalainila, P., Subha, V., Ravindran, R. S. E., & Renganathan, S. (2014). SYNTHESIS AND

344   CHARACTERIZATION OF SILVER NANOPARTICLE FROM Erythrina indica. *Asian J*

345   *Pharm Clin Res*, *7*(2), 39–43.

346   Kaviya, S., Santhanalakshmi, J., & Viswanathan, B. (2011). Green synthesis of silver

347   nanoparticles using Polyalthia longifolia leaf extract along with D-sorbitol: Study of

348   antibacterial activity. *J Nanotech*, *2011*. https://doi.org/10.1155/2011/152970

349   Lantero, A. (2014). Sewarine, an indole alkaloid from Rhazya stricta and a κ opioid receptor

350   antagonist, induces apoptosis via caspase activation in various cancer cell lines, and inhibits

351   NF-κB activation. *Intrinsic Activity*, *2*(Suppl. 1), A1.20. https://doi.org/10.25006/IA.2.S1-

352   A1.20

353   Li, G., He, D., Qian, Y., Guan, B., Gao, S., Cui, Y., … Wang, L. (2012). Fungus-mediated green

354   synthesis of silver nanoparticles using aspergillus terreus. *Int. J. Mol. Sci*, *13*(1), 466–476.

355   https://doi.org/10.3390/ijms13010466

356   Logeswari, P., Silambarasan, S., & Abraham, J. (2015). Synthesis of silver nanoparticles using

357   plants extract and analysis of their antimicrobial property. *J. Saudi Chem. Soc.*, *19*(3), 311–

358   317. https://doi.org/10.1016/j.jscs.2012.04.007

359   Nasir, G. A., Mohammed, A. K., & Samir, H. F. (2016). Biosynthesis and Characterization of

360   Silver Nanoparticles Using Olive Leaves Extract and Sorbitol. *Iraqi J Biotech*, *15*(1), 22–

361   32.

362   Nehdi, I. A., Sbihi, H. M., Tan, C. P., & Al-Resayes, S. I. (2016). Seed oil from Harmal (Rhazya

363   stricta Decne) grown in Riyadh (Saudi Arabia): A potential source of δ-tocopherol. *J Saudi*

364   *Chem Soc*, *20*(1), 107–113. https://doi.org/10.1016/j.jscs.2014.09.005

365   Obaid, A. Y., Voleti, S., Bora, R. S., Hajrah, N. H., Omer, A. M. S., Sabir, J. S. M., & Saini, K.

366   S. (2017). Cheminformatics studies to analyze the therapeutic potential of phytochemicals

367   from Rhazya stricta. *Chem Cent J*, *11*(1), 1–21. https://doi.org/10.1186/s13065-017-0240-1

368   Painuli, R., Joshi, P., & Kumar, D. (2018). Cost-effective synthesis of bifunctional silver

369   nanoparticles for simultaneous colorimetric detection of Al(III) and disinfection. *Sensors*

370   *and Actuators, B: Chemical*, *272*(February), 79–90.

371   https://doi.org/10.1016/j.snb.2018.05.131

372   Ponarulselvam, S., Panneerselvam, C., Murugan, K., Aarthi, N., Kalimuthu, K., & Thangamani,

373   S. (2012). Synthesis of silver nanoparticles using leaves of Catharanthus roseus Linn. G.

374   Don and their antiplasmodial activities. *Asian Pac J Trop Biomed*, *2*(7), 574–580.

375   https://doi.org/10.1016/S2221-1691(12)60100-2

376   Rajasekharreddy, P., & Rani, P. U. (2014). Biofabrication of Ag nanoparticles using Sterculia

377   foetida L. seed extract and their toxic potential against mosquito vectors and HeLa cancer

378   cells. *Mater. Sci. Eng. C*, *39*(1), 203–212. https://doi.org/10.1016/j.msec.2014.03.003

379   Rauf, Abdul, Ajmal Khan, Zara Dawood, Ghias Uddin, Umar Farooq AM. 2016. Synthesis,

380   Characterization and Bioactivities of Silver Nanoparticles using Ethanolic and Aqueous

381   Extracts of Rhazya strictica. In: *NanosmatAt: The University of Texas at Arlington, Texas,*

382   *USA*. 1–704.

383   Saiqa Ikram, S. A. (2015). Silver Nanoparticles: One Pot Green Synthesis Using Terminalia `

384   Arjuna   Extract   for   Biological   Application.   *J   Nanomed   Nanotech*,   *6*(4).

385   https://doi.org/10.4172/2157-7439.1000309

386   Sana, S. S., & Dogiparthi, L. K. (2018). Green synthesis of silver nanoparticles using Givotia

387   moluccana leaf extract and evaluation of their antimicrobial activity. *Materials Letters*, *226*,

388   47–51. https://doi.org/10.1016/j.matlet.2018.05.009

389   Sarfaraz Khan Marwat. (2012). A review of phytochemistry, bioactivities and ethno medicinal

390   uses of Rhazya stricta Decsne (Apocynaceae). *Afr J Microbiol Res*, *6*(8), 1629–1641.

391   https://doi.org/10.5897/AJMRx11.024

392   Singh, M., Singh, S., Prasad, S., & Gambhir, I. S. (2008). Nanotechnology in Medicine and

393   Antibacterial Effect of. *Dig J Nanomater Biostruct*, *3*(3), 115–122. Retrieved from

394   http://tse.colloidalsilverkillsviruses.com/pdf/n HYPERLINK

395   Singh, P., Kim, Y. J., Wang, C., Mathiyalagan, R., & Yang, D. C. (2016). The development of a

396   green approach for the biosynthesis of silver and gold nanoparticles by using Panax ginseng

397   root extract, and their biological applications. *Artif Cells Nanomed Biotechnol*, *44*(4), 1150–

398   1157. https://doi.org/10.3109/21691401.2015.1011809

399 Van Beek, T. A., Verpoorte, R., Svendsen, A. B., & Fokkens, R. (1985). Antimicrobially active

400   alkaloids from tabernaemontana chippii. *J. Nat. Prod*, *48*(3), 400–423.

401   https://doi.org/10.1021/np50039a008

402 Verma, A., & Mehata, M. S. (2016). Controllable synthesis of silver nanoparticles using Neem

403   leaves and their antimicrobial activity. *J Radiat Res Appl Sc*, *9*(1), 109–115.

404   https://doi.org/10.1016/j.jrras.2015.11.001

405 Wang, D., Markus, J., Wang, C., Kim, Y.-J., Mathiyalagan, R., Aceituno, V. C., … Yang, D. C.

406   (2017). Green synthesis of gold and silver nanoparticles using aqueous extract of Cibotium

407   barometz root. *Artif Cells Nanomed Biotechnol*, *45*(8), 1548–1555.

408   https://doi.org/10.1080/21691401.2016.1260580

409

410 **Figure Legends**

411 **Figure 1**: Schematic presentation of methodology for synthesis of AgNPs with root extract of

412 *Rhazya stricta.*

413 **Figure 2**: **(A)** Change in color after synthesis of AgNPs. **(B)** Concentration dependent UV-Vis

414 Spectra of AgNPs of *Rhazya stricta*.

415 **Figure 3**: SEM showing spherical AgNPs. **(A)** AgNPs of plant extract only **(B)** AgNPs of plant

416 extract with xylitol

417 **Figure 4**: Energy Dispersive X-Ray image of AgNPs synthesized using *Rhazya stricta.*

418 **Figure 5**: X-Ray Diffraction (XRD) image of the AgNPs synthesized using *Rhazya stricta.*

419   **Figure 6**: (**A**) FTIR of Xylitol. (**B**) FTIR of medicinal plant Rhazya stricta. (**C**) FTIR of AgNPs

420   using *Rhazya stricta.* (**D**) FTIR of AgNPs using *Rhazya stricta* along with xylitol.

421   **Figure 7**: (**A**) Concentration dependent effect of *Bacillus subtilis.* (**B**) Graphical presentation for

422   concentration dependent effect of *Bacillus subtilis.* (**C**) Concentration dependent effect of

423   *Escherichia coli.* (**D**) Graphical presentation for concentration dependent effect of *Escherichia*

424   *coli*.

425   **Figure 8**: (**A**) Time dependent effect of *Bacillus subtilis.* (**B**) Graphical presentation for time

426   dependent effect of *Bacillus subtilis*. (**C**) Time dependent effect of *Escherichia coli.* (**D**) Graphical

427   presentation for time dependent effect of *Escherichia coli*.

428   **Figure 9**: (**A**) Difference between effect of silver nanoparticles of R. stricta along with xylitol on

429   *Escherichia coli* and *Bacillus subtilis*. (**B**) Graphical presentation for comparative effect of AgNPs

430   against *Escherichia coli* and *Bacillus subtilis.*

Figure 1

Methodology for synthesis of AgNPs

Schematic presentation of methodology for synthesis of AgNPs with root extract of *Rhazya stricta.*
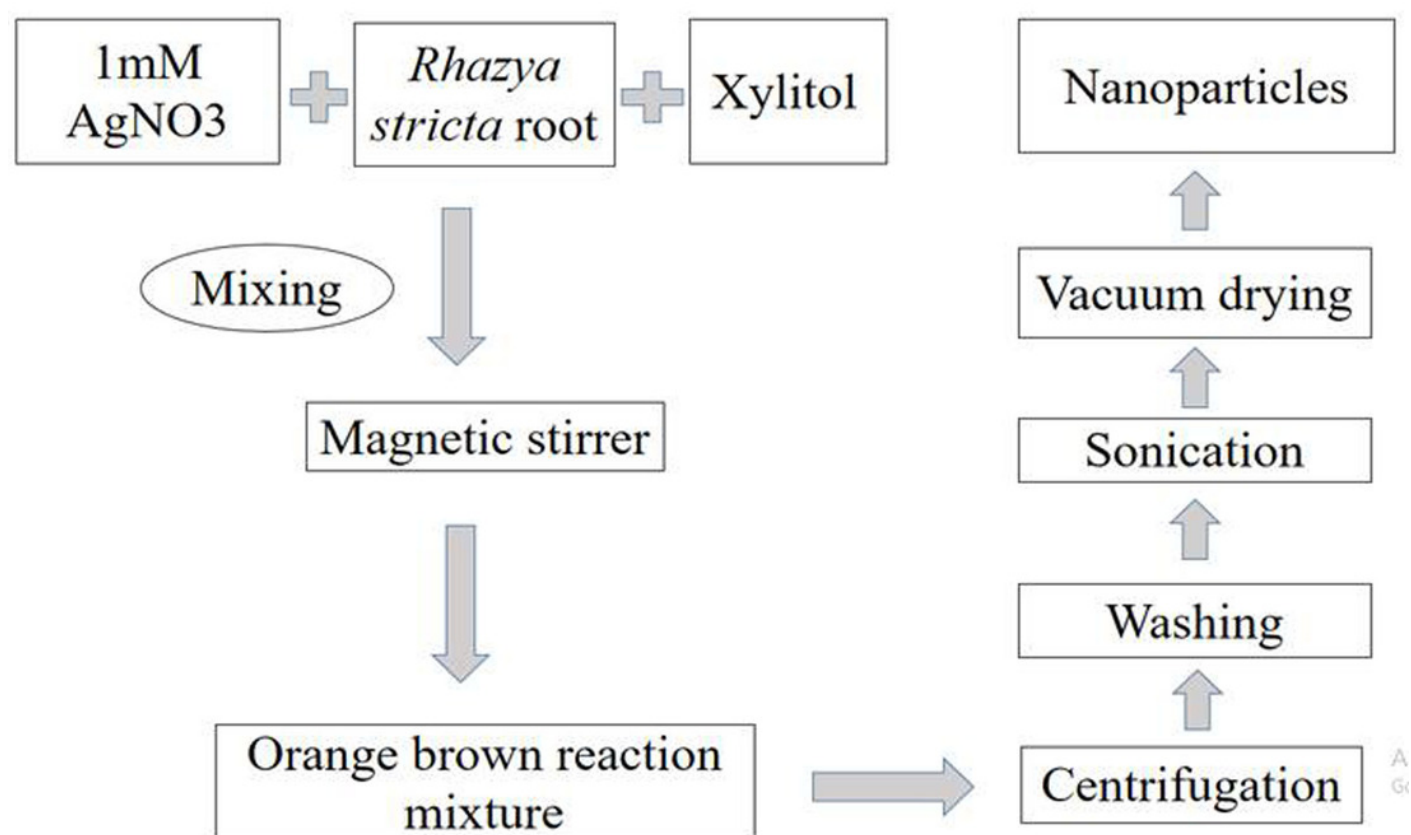
Figure 2

Charecterization of AgNPs

(A) Change in color after synthesis of AgNPs. **(B)** Concentration dependent UV-Vis Spectra of AgNPs of *Rhazya stricta*.

Photo credit: Saima Jabeen
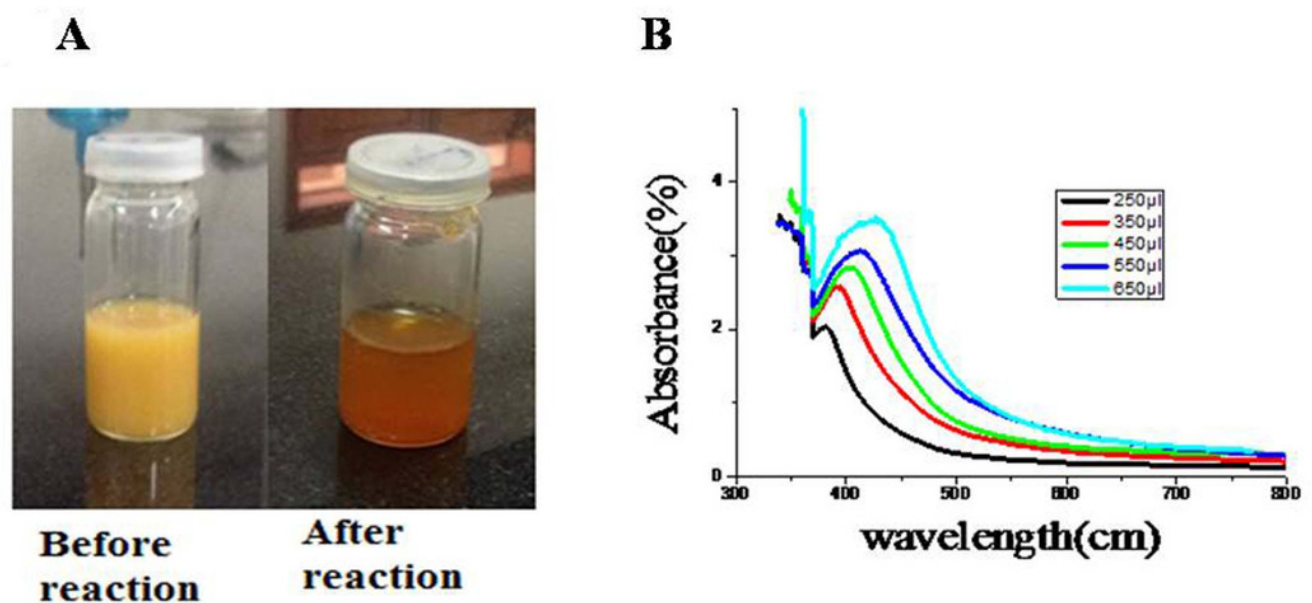
Figure 3

SEM images of AgNPs

(A) AgNPs of plant extract only (B) AgNPs of plant extract with xylitol
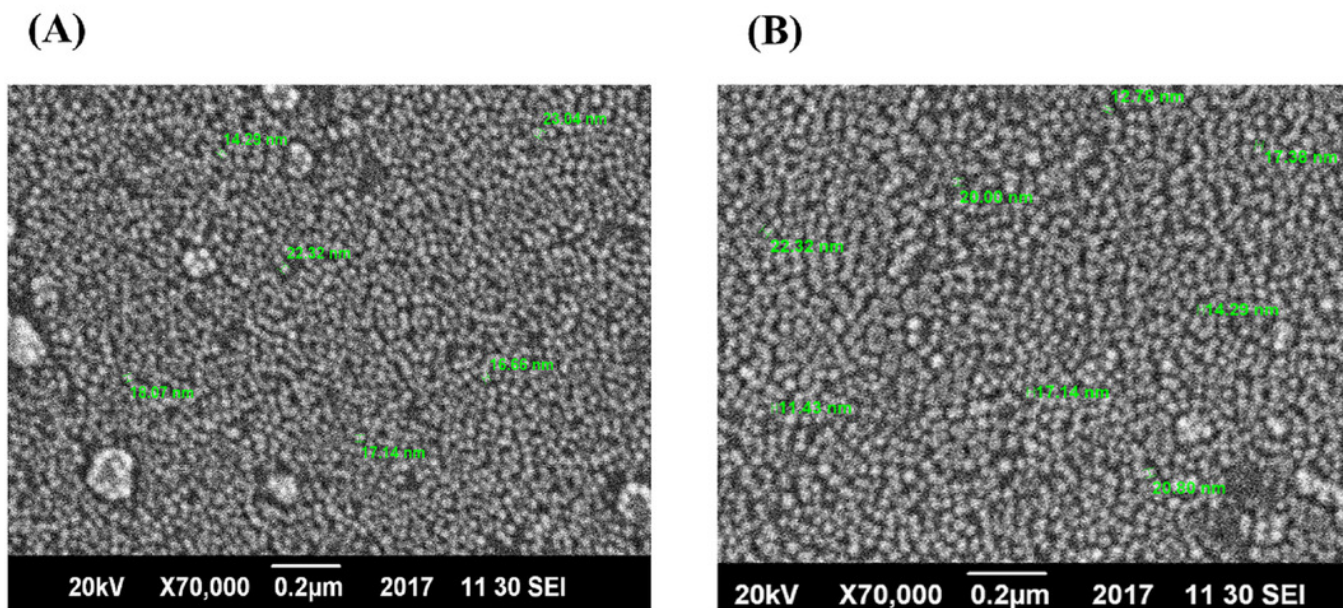
Figure 4

EDX spectrum

Energy Dispersive X-Ray image of AgNPs synthesized using *Rhazya stricta*
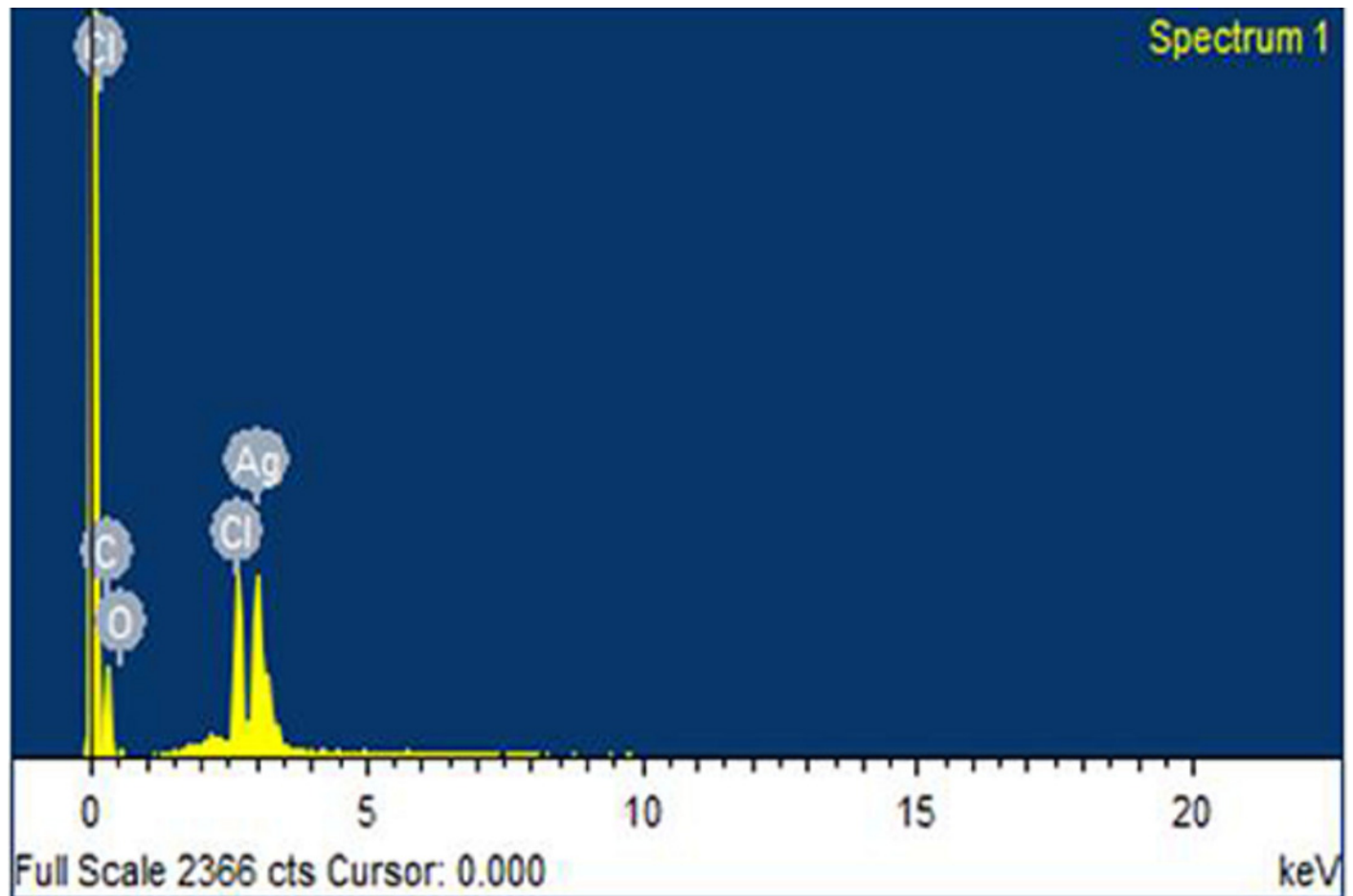
Figure 5

XRD patterens

X-Ray Diffraction (XRD) image of the AgNPs synthesized using *Rhazya stricta*
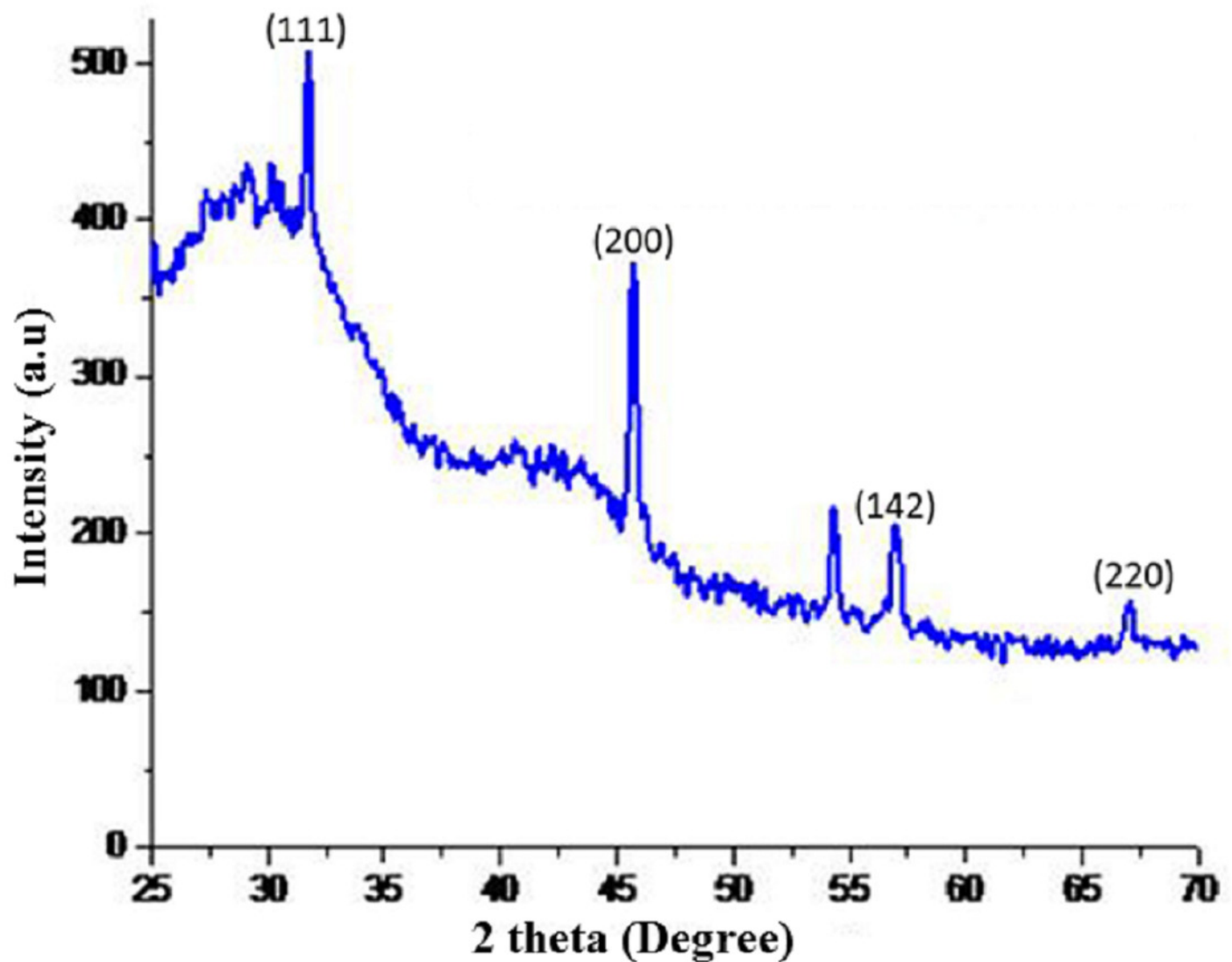
Figure 6

FTIR spectrum

(**A**) FTIR of Xylitol. (**B**) FTIR of medicinal plant R. stricta. (**C**) FTIR of AgNPs using *Rhazya stricta.* (**D**) FTIR of AgNPs using *Rhazya stricta* along with xylitol

(A)

FTIR of Xylitol

(B)

FTIR of medicinal plant *Rhazya stricta*

(C)

FTIR of silver nanoparticles of *Rhazya stricta*

(D)

FTIR of silver nanoparticles of *Rhazya stricta* along with Xylitol
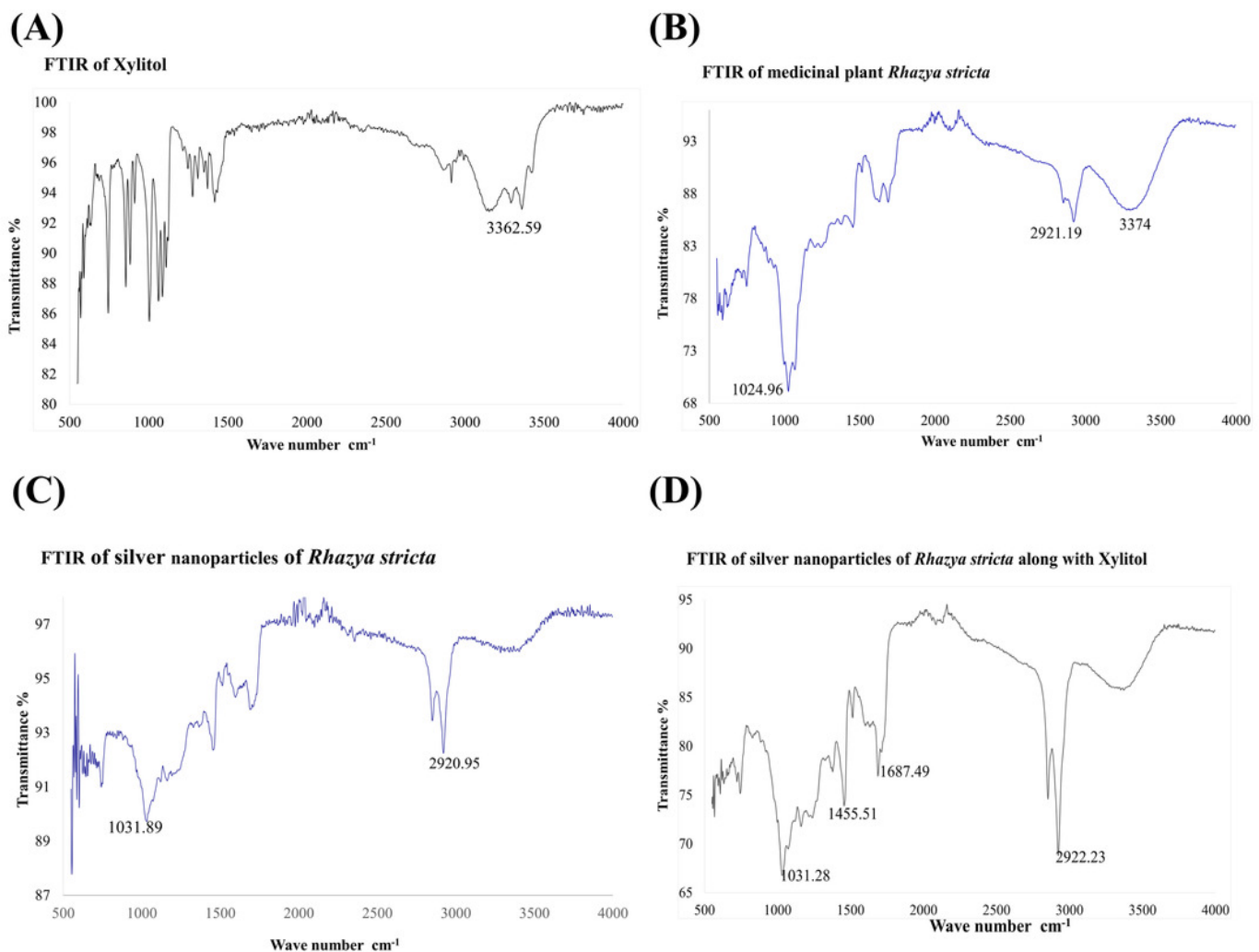
Figure 7

Concentration dependent antimicrobial activity of Ag NPs

(**A**) Concentration dependent effect of *Bacillus subtilis.* (**B**) Graphical presentation for concentration dependent effect of *Bacillus subtilis*. (**C**) Concentration dependent effect of *Escherichia Coli.* (**D**) Graphical presentation for concentration dependent effect of *Escherichia Coli*
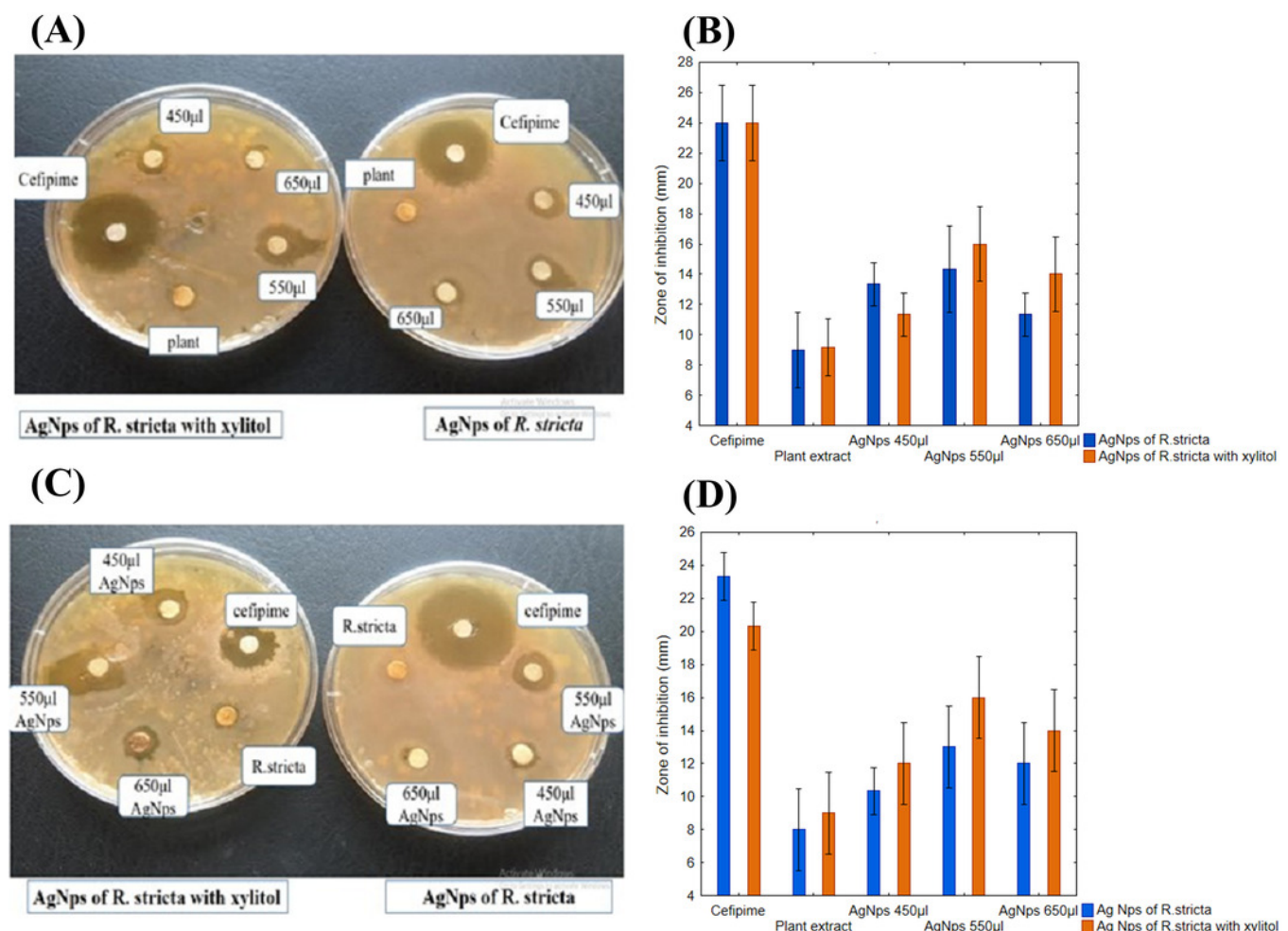
Figure 8

Time dependent antimicrobial activity of AgNPs

(**A**) Time dependent effect of *Bacillus subtilis.* (**B**) Graphical presentation for time dependent effect of *Bacillus subtilis*. (**C**) Time dependent effect of *Escherichia Coli.* (**D**) Graphical presentation for time dependent effect of *Escherichia Coli*
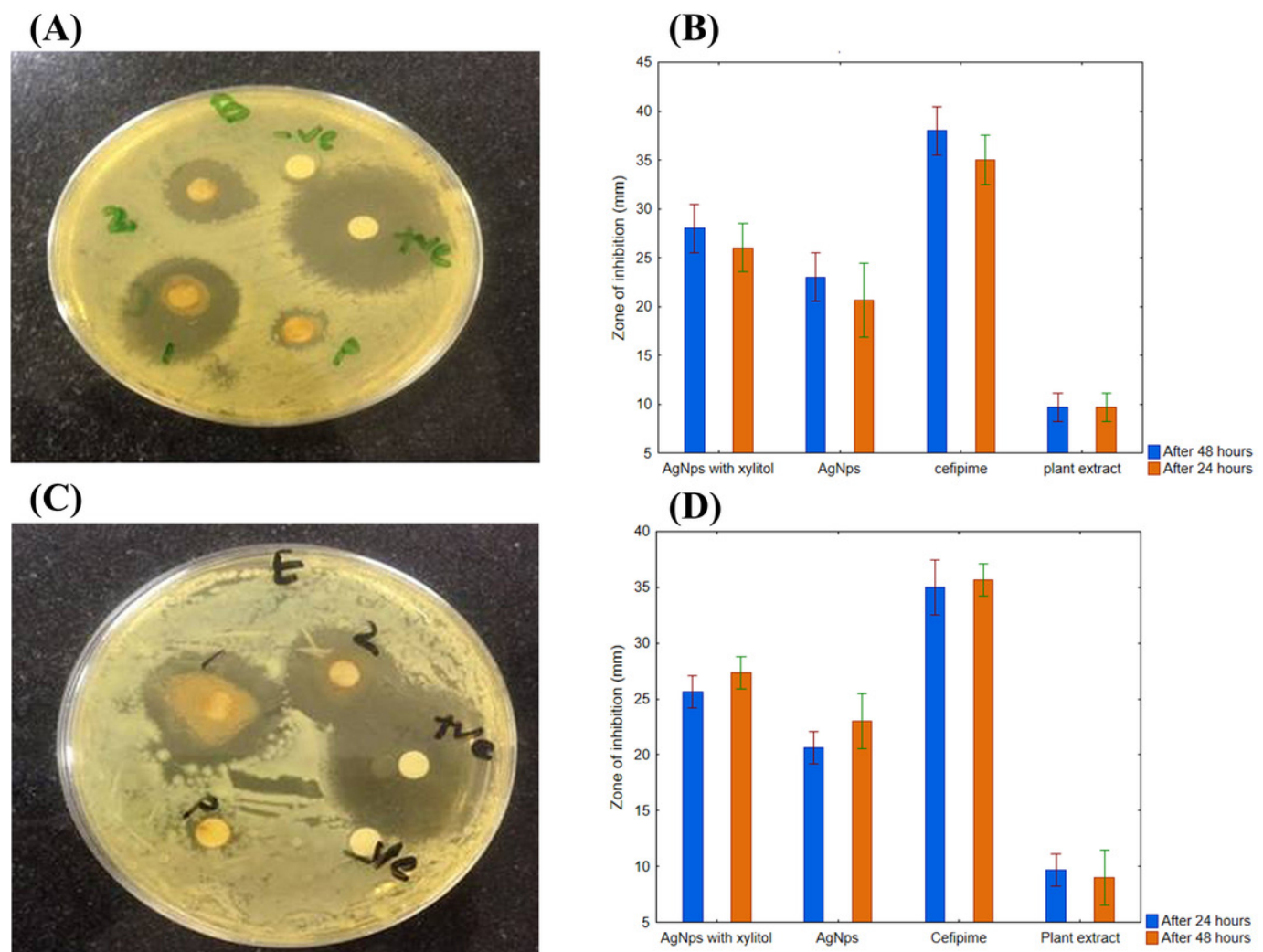
Figure 9

comparative effect of AgNPs against *Escherichia Coli* and *Bacillus subtilis.*

(A) Difference between effect of silver nanoparticles of R. stricta along with xylitol on *Escherichia Coli* and *Bacillus subtilis*. (B) Graphical presentation for comparative effect of AgNPs against *Escherichia Coli* and *Bacillus subtilis.*